The warp of the Galaxy and the Large Magellanic Cloud

Garcia-Ruiz, I.; Kuijken, K.; Dubinski, J.

Published in:
Monthly Notices of the Royal Astronomical Society

DOI:
10.1046/j.1365-8711.2002.05923.x

Mon. Not. R. Astron. Soc. **337,** 459–469 (2002)

The warp of the Galaxy and the Large Magellanic Cloud

I. García-Ruiz,[1] K. Kuijken[1⋆] and J. Dubinski[2]

[1] *Kapteyn Astronomical Institute, PO Box 800, 9700 AV, Groningen, the Netherlands*
[2] *Canadian Institute for Theoretical Astrophysics, 60 St George St., M5S 3H8 Toronto, Canada*

Accepted 2002 July 29. Received 2002 July 19; in original form 2000 February 14

ABSTRACT

We study the possibility that the Galactic warp is caused by the tides of the Magellanic clouds. Using a specialized *N*-body particle+ring code we investigate the role of extra torques on the disc induced by gravitational wakes in the dark halo created by the Large Magellanic Cloud. We find that neither the amplitude nor the orientation of the resulting warp agrees with observations.

Key words: Galaxy: structure – galaxies: kinematics and dynamics – Magellanic Clouds.

1 INTRODUCTION

In many spiral galaxies the outer regions of the disc warp away from the symmetry plane of the inner disc, often resembling an integral sign. Early studies on warps showed that this is a very common phenomenon (Sancisi 1976), and later this was confirmed in bigger samples (Sánchez-Saavedra, Battaner & Florido 1990; Bosma 1991). From the beginning this presented dynamicists with a difficult puzzle. The presence of warps in most of the galaxies suggests that either warps are continuously being excited, or they have survived for a long time since they were generated. The first scenario needs a perturbing agent to warp the disc more or less continuously, while the second needs a way of maintaining a coherent pattern against the destructive effects of differential precession.

Sparke & Casertano (1988) studied long-lived warping normal modes inside an oblate halo potential, where no winding occurs. They calculated long-lived modes but failed to consider the halo as a responding potential that would react to the disc. When Dubinski & Kuijken (1995) and Nelson & Tremaine (1995), following a comment by Toomre (1983), considered the response of the halo to the gravity of the disc, and analysed how this affected the disc, they discovered that those modes damped too quickly.

Most recent work has focused on one of the following possibilities: (i) warps are caused by infalling clumps of dark matter that re-orient the haloes, as a result of which a disc warp is induced (Ostriker & Binney 1989; Ing-Guey & Binney 1999); (ii) an angular momentum misalignment between the halo and the disc excites a warp (Debattista & Sellwood 1999); (iii) satellites orbiting the warped galaxy cause a warp by tidal interaction with its disc.

This paper is concerned with the satellite-forcing scenario. The crucial issue is how to enhance the tides directly exerted by the satellites on to the galaxy disc into a perturbation sufficiently strong to generate the observed warps. Usually the satellite galaxies that are found orbiting warped galaxies are not massive enough to account for the warp amplitudes observed. For example, the Galactic warp could not be generated by the direct tidal forcing of the Large Magellanic Cloud (LMC) at its present distance, because its influence is too weak (Burke 1957; Kerr 1957; Hunter & Toomre 1969).

Weinberg (1998) describes a calculation in which a disc galaxy surrounded by a dark halo is perturbed by a massive satellite, similar to the LMC. By means of a linear perturbation analysis, he follows the perturbation (wake) created by the satellite in the halo, including its self-gravity. He finds that the torque exerted by this wake on the disc is several times larger than that due directly to the satellite. The latter is amplified because: (i) the satellite-induced wake in the halo itself exerts a torque, roughly in phase with that from the satellite and (ii) the wake itself further perturbs the halo, resulting in a torque that is larger again. As Weinberg shows, the details of the disc model (and hence its vertical oscillation mode spectrum) sensitively determine the degree of warping in response to the satellite and halo wake perturbations. The amplification of the satellite tidal effect on the disc by a wake was originally addressed in a calculation by Lynden-Bell (1985) of a similar scenario, as well as in a simple model described by Kuijken (1997).

Weinberg's calculation, while impressive, relies on a number of simplifying assumptions, as follows.

(i) The halo model is taken to be a King model, i.e. to be spherical and radially scale-free over a substantial radial range. The symmetry reduces the dimensionality of phase space, making the calculation of the response of the halo more tractable. However, real galaxies will have haloes that are somewhat flattened by their discs, and which are not scale-free.

(ii) The response of the disc is calculated after that of the halo is established, i.e. the backreaction of the disc on the halo is ignored. However, as shown by Dubinski & Kuijken (1995) and Nelson & Tremaine (1995) disc damping against the halo is an important effect.

(iii) The satellite orbit is taken to be quasi-periodic, as is appropriate for a non-decaying orbit. However, a satellite massive enough to warp the disc will be affected by dynamical friction, and hence will have a decaying orbit.

(iv) Only the steady-state forced response is calculated, not the transient responses. Since satellite orbital frequencies are rather low

⋆E-mail: kuijken@strw.leidenuniv.nl

(the orbital period of the LMC is about 1.5 Gyr) the transients may be important.

In this paper we investigate these questions by means of *N*-body simulations. Section 2 contains a description of the *N*-body code used and Section 3 contains the results of our simulations: there we show that the amplification by the halo wake in our model is modest. In Section 4 we present a simple model that predicts the orientation of the line of nodes of the warp for a polar satellite. In Section 5 we give our conclusions.

2 SIMULATION DETAILS

2.1 *N*-body ring code

The *N*-body code used to evolve the system uses a hybrid approach. The halo is modelled using particles while the disc is modelled using a system of concentric, spinning rings. The gravitational potential of the halo is computed using a self-consistent field (SCF) code (Hernquist & Ostriker 1992), expanding the potential in terms of radial (quantum number n) and spherical harmonic (numbers l, m) basis functions. Basis functions up to $n=6$, $l=4$ were used in this paper. We have made several checks to make sure that we have used high enough harmonics in our expansion. We have compared the particle density directly determined from the particle halo (Fig. 4 in Section 3.4) with the truncated expansion used by the SCF code for the same halo (Fig. 5 in Section 3.4). The match shows us that an expansion up to $n=6$, $l=4$ is able to resolve the wakes generated by the satellites in the halo with sufficient accuracy (the imaging of the wake is explained in detail in Section 3.4). As a double check, we also run some simulations with higher harmonics ($n=6$, $l=8$), and no significant variation in either the warp nor in the wake was detected.

The disc is treated as a system of spinning rings centred on the halo. The rings are spaced uniformly but have varying mass to represent the disc density profile. Each ring is realized as 36 equal-mass particles that are azimuthally equally spaced. The gravitational potential generated by the ring particles are calculated using a tree code (Barnes & Hut 1986) since the SCF method cannot determine the potential accurately for highly flattened systems. The gravitational forces on these individual 'ring particles' are then used to calculate the torque on each ring, which were used in the solution of Euler's equations.

Finally, we treated satellites as single particles with a Plummer-law potential. The force exerted by a satellite on the simulation particles was evaluated directly using the Plummer potential while the satellite moved under the influence of the halo and disc potentials.

We simultaneously integrate the equations of motion for the halo particles and the system of Euler's equations for the rigid-ring system describing the disc. The total energy and angular momentum of the combined particle and ring system were found to well conserved with typical errors less than 1 per cent in these quantities by the end of a typical simulation.

2.2 Initial conditions

To simulate the tidal amplification of a satellite by a halo we have chosen a set of initial conditions following Weinberg (1998). We have adopted as a halo the one that generated the greatest warp in his calculations, as well as an exponential disc with a scalelength of 4.5 kpc. The disc is exponential except by 5 scalelengths, and then it is tapered smoothly to zero over the last scalelength as described in Kuijken & Dubinski (1995).

The units of the model translate to the Galaxy (disc scalelength of 4.5 kpc and a rotation velocity at 8.5 kpc of 220 km s^{-1}) as follows: length unit = 4.5 kpc, velocity unit = 315 km s^{-1}, time unit = 1.40×10^7 yr, mass unit = 1.03×10^{11} $M_\odot$. With these numbers, the disc mass of our model is 5.24×10^{10} $M_\odot$, and the satellite (LMC) has a mass of 1.5×10^{10} $M_\odot$, the (highest current mass estimate for the Clouds; see Schommer et al. 1992). In the coordinate system of the simulations, $z=0$ is the disc plane, and the orbit of the satellite lies in the $x=0$ plane.

We have used two different types of simulations: semilive and live. In the 'semilive' simulations, the effect of the disc on the halo is suppressed. The halo model used for these simulations is a King model with $\Psi_0/\sigma_0^2=-6$, a tidal radius of 44 and a mass of 10 disc masses (see Fig. 1 for the mass profile and the rotation curve). We use this halo for the simulations in which the effect of the disc on the halo is suppressed.

In the 'live' simulations the halo is allowed to feel the effects of the disc. Here the initial conditions need to be different, as our King model halo and the exponential disc are obviously not in equilibrium. Hence for these runs we have allowed our halo to relax prior to the run. For this purpose we evolved the King halo with a disc, forcing the disc to remain flat in the initial configuration until the system does not evolve any further. Once the halo and disc have relaxed, we introduce the satellite and allow the disc to depart from the disc plane. Letting the halo relax in the presence of the disc causes the density to increase in the internal parts of the halo, which makes the contribution of the halo to the rotation curve higher in the inner parts. It peaks higher (by $\simeq$20 per cent) and at a smaller radius (25 per cent) than before.

For each model we used $N_{\rm h}=500\,000$ particles for the halo and 600 rings for the disc. Each ring contained 36 particles. Various runs where made with more rings and more particles per ring, without significant changes in the results described below. We also made a simulation with 5 000 000 particles for the halo (simulation no 4, described in Section 3.3) and obtained the same results.

We use two Plummer-law satellites, symmetrically placed with respect to the centre of the halo–disc system to nullify the dipole term of the tidal field. In this way, we avoid relative movements of the galaxy with respect to the satellites and focus on the quadrupole ($l=2$) terms that dominate in generating the warp.

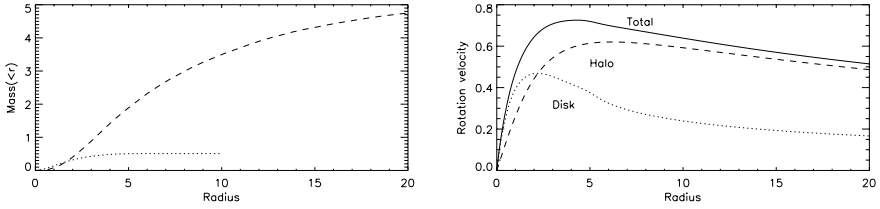

Figure 1. Mass profile and rotation curve: disc (dotted), halo (dashed) and total (solid). Simulation units are described in Section 2.2.

Table 1. Summary of all the simulations used in this article (the standard simulation is in bold). (1) See Section 2.2, (2) Assuming $M_{\rm LMC} = 1.5 \times 10^{10}$ M$_\odot$, (3) number of halo particles, (4) sense of rotation of the orbit, (5) the satellite orbit allowed to decay under dynamical friction? (6) the halo allowed to respond to the satellite (form a wake)? (7) the halo allowed to respond to the disc?

No	Halo model (1)	$M_{\rm sat}/M_{\rm LMC}$(2)	$N_{\rm halo}$ (3)	$Lx_{\rm sat}$ (4)	Dyn. Fr. (5)	Sat → Halo (6)	Disc → Halo (7)
1	King	0	500 000	–	–	–	No
2	King	1	500 000	–	No	No	No
3	**King**	**1**	**500000**	–	**No**	**Yes**	**No**
4	King	10	5 000 000	–	No	Yes	–
5	King	10	500 000	–	No	No	No
6	King	10	500 000	–	No	Yes	No
7	King	10	500 000	+	No	Yes	No
8	King relaxed	0	500 000	–	–	–	Yes
9	King relaxed	10	500 000	–	Yes	Yes	Yes

The simulations begin with the satellite at its apocentre where the density of the halo is lowest, to minimize disturbance to the equilibrium halo–disc model and give enough time for the halo to develop a gravitational wake caused by the satellite, before it gets to its pericentre.

The satellites are placed in a polar orbit with pericentre at 50 kpc and apocentre at 100 kpc, consistent with a recent determination of the orbit of the Clouds (Lin, Jones & Klemola 1995). In the first simulations dynamical friction is suppressed but incorporated later when the response of the halo to the disc is computed (Section 3.6). The orbit of the satellite in the case where dynamical friction is neglected is shown in Fig. 2.

Our standard model consists of the exponential disc, the King model halo, and the satellite orbiting in the 50–100 kpc non-decaying orbit recently described. All simulations were run for 320 time units (which corresponds to 4.5 Gyr).

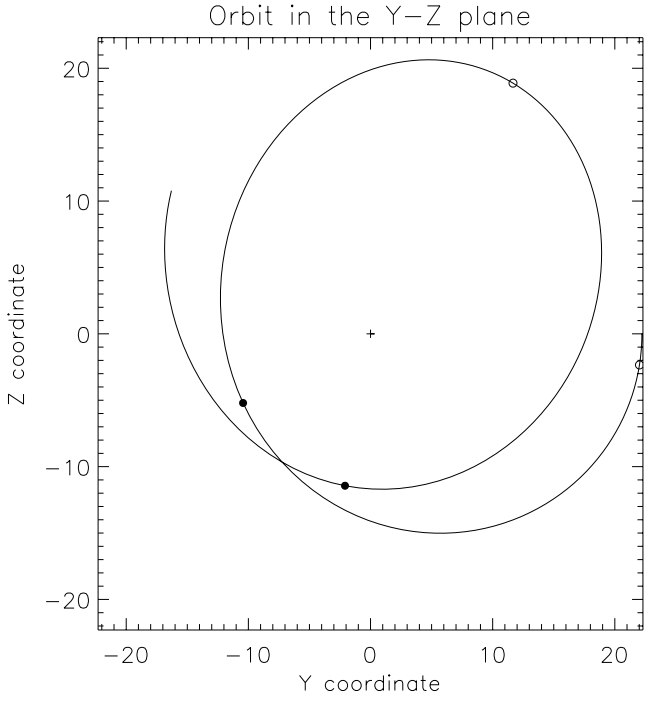

Figure 2. Orbit of one of the pair of satellites (the other one orbits symmetrically) used in simulations nos 2–6 (without dynamical friction). We have plotted the trajectory in the plane of the orbit and indicated the apogalacticon and perigalacticon with empty and filled circles, respectively. The period of the satellite is 88.6 time units.

3 RESULTS

We have performed a number of simulations to look for the effect described in Weinberg (1998). We first simulate a system resembling the Galaxy and LMC and later increase the mass of the satellite to observe the warp above our particle noise level. For a summary of all the simulations performed, see Table 1

3.1 Control simulation

We first simulated our standard model parameters for the disc and the halo but without satellites (simulation no 1) to determine any disc warping from particle noise. We find that the particle noise caused by the halo had excited a warp in the disc with an amplitude of 3.5° at $r = 6$.

3.2 Semilive halo

In this section, we calculate the bending of the disc caused by orbiting satellites by switching off the effect of the disc on the halo (and hence its backreaction on the disc), in an effort to reproduce Weinberg's calculations.

First, we switch off the effect of the satellite on the halo as well (simulation no 2), to quantify the warp amplitude in the case of only direct tidal forcing by the satellite. This simulation shows warp amplitudes that are indistinguishable from the control simulation, indicating that the raw tidal field of the satellite is much too weak to affect the disc.

The standard model (resembling the LMC–Galaxy, simulation no 3), including the effect of the satellite on the halo develops a warp no bigger than 0.5° above the control simulation.

The wake that is created in our halo as a result of the perturbed satellite peaks inside the orbit of the satellite, but not as deeply as half the distance (2 : 1 resonance mentioned in Weinberg 1998). Since tides depend strongly on distance, this more distant wake results in insufficient amplification of the tidal effect on the disc.

3.3 High-resolution halo simulation and massive satellites

We tried to detect the wake in the halo by comparing simulations 2 and 3 but particle noise is too high to detect the small wake in our halo. We address this problem of resolution using two approaches. First, we performed a higher-resolution simulation with 5×10^6 particles in the halo (an order of magnitude higher than our standard simulations) of a satellite orbiting a halo (simulation no 4) using a parallel tree code (Dubinski 1996). We do not include a disc in

this simulation, which otherwise had the same initial conditions as simulation no 3.

We have also run simulations with the same initial conditions as in simulations 2 and 3 but with a satellite that is an order of magnitude more massive (1.5×10^{11} $M_{\odot}$). We again performed a simulation including only the direct tidal forcing of the satellite on the disc (simulation no 5) and another one including the influence of the satellite on the halo (simulation no 6).

We keep the satellite in the same orbit as in simulations 2 and 3 but allow the halo to respond to the more massive satellite to induce a stronger wake in the halo. We do not let the satellite orbit evolve self-consistently since otherwise the satellite would spiral into the galaxy in a time-scale shorter than the Hubble time.

If the wake in the halo is still in the linear perturbation regime, we would expect the wake (and therefore the torque on the disc) of the high-resolution simulation to be an order of magnitude smaller than that of simulation no 6 (because the wake scales linearly with the mass of the satellite).

We compared simulations 4 and 6 by computing the torque that the halo (with the wake created by the satellite) would create on a flat disc. We then compared it with the direct torque that the disc feels from the satellite. Fig. 3 shows these torques for both simulations. The first conclusion we derive from this figure is that both simulations agree at an excellent level in the contribution of the wake to the total torque, which is not larger than 25 per cent. The fact that the wakes in the 5×10^6 particle halo are producing the same amount of torque on a disc suggests that we are converging to the correct dynamical behaviour.

Thus, even if the halo does contribute to the torque that a disc experiences from a satellite, this extra contribution is quite modest. Note as well that the torque generated by the wake on the halo is not exactly in phase with the torque arising directly from the satellite.

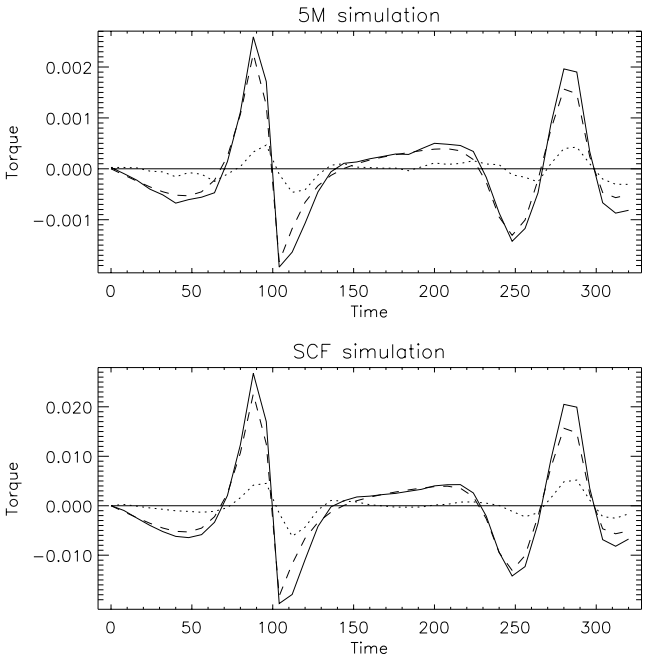

Figure 3. Torques on a flat disc caused by the satellite (dashed line), the halo (dotted line) and the total torque (solid line). The upper plot shows torques calculated from the high-resolution simulation (simulation no 4), while the plot at the bottom shows the SCF simulation results (simulation no 6, with a satellite 10 times more massive and a factor of 10 fewer halo particles than simulation no 4).

The wake is slightly behind the satellite, which causes the torque from the wake to peak some time after the torque from the satellite. This will make the combined torque from both wake and satellite smaller than the sum of both, so we expect the warp amplitudes not to be increased by more than 25 per cent when the wake is taken into account.

The comparison between the high-resolution simulation and simulation no 6 also indicates that the SCF simulations accurately represent the satellite–halo interaction, and that we can use them to explore the properties of warps in halo–satellite–disc systems.

3.4 The wake and the satellite

We have compared simulations 5 (no wake) and 6 (wake) to estimate the contribution of the wake to the warping of the disc.

The difference in the warping of the disc between simulations nos 5 and 6 is the warping induced by the wake in the halo on the disc. If this effect is very important we would expect larger warps in simulation no 6. In agreement with the lower-mass satellite simulations (nos 2 and 3) and torque calculations in Fig. 3, the disc warp obtained is less than 20 per cent larger in simulation no 6 than in no 5, indicating that the wake in the halo contributes only a fraction of the torque exerted by the satellite itself.

We then attempted to image the wake in the halo by subtracting the estimated halo density from the particle distribution simulation no 5 (no wake) from that of simulation no 6 (wake included). Contour plots of the halo density in the orbital plane are shown in Fig. 4. We have also calculated the wake in density comparing the SCF expansions for both simulations (Fig. 5). The wake follows the satellite from behind clearly along the simulation, having its maxima at a smaller radius than where the satellite is. Even if we lack resolution to tell exactly where the maxima of the wake are (these maps are smoothed), it is further out than half the orbital radius of the satellite. This smoothing has to be taken into account when comparing Figs 4 and 5. If we smoothed the density plots of Fig. 5, the peak of the wake would shift outwards in radius.

3.5 Halo particle noise

As a check on the influence of particle noise on our results, we performed another simulation (simulations no 7) with the same parameters as no 6 but with the orbit of the satellites having opposite angular momentum ($z_{\rm sim6} = -z_{\rm sim7}$). In the absence of halo particle noise, we would obtain the same warp amplitude in both simulations, with a difference in the position angle of the line of nodes of 180°. On the other hand, if we see that the line of nodes of simulation no 7 is close to that of no 6, this means that the noise from halo discreteness is dominating the warp.

The warps of both simulations are shown in Figs 6 and 7, where we have plotted tip-LON diagrams (Briggs 1990) at different timesteps for these two simulations. We have computed the line of nodes averaging the disc every 50 rings (0.5 scalelengths). In these plots we can see that up to $t = 160$ the effect from the wake and the satellite is dominant, but after this the halo particle noise grows, dominating the shape (and orientation) of the warp.

At the end of the simulation ($t = 320$), the maximum amplitude of the warp at 6 scalelengths is smaller than 6°. This poses an upper limit to the warp generated by the satellite and the halo wake, since the noise-excited warp is the main driver of the warp we see. If the warp excited by the satellite–halo system were as important as the noise-excited one we would detect differences in the final warp of simulations nos 5 and 6, which we do not. If we find a maximum warp

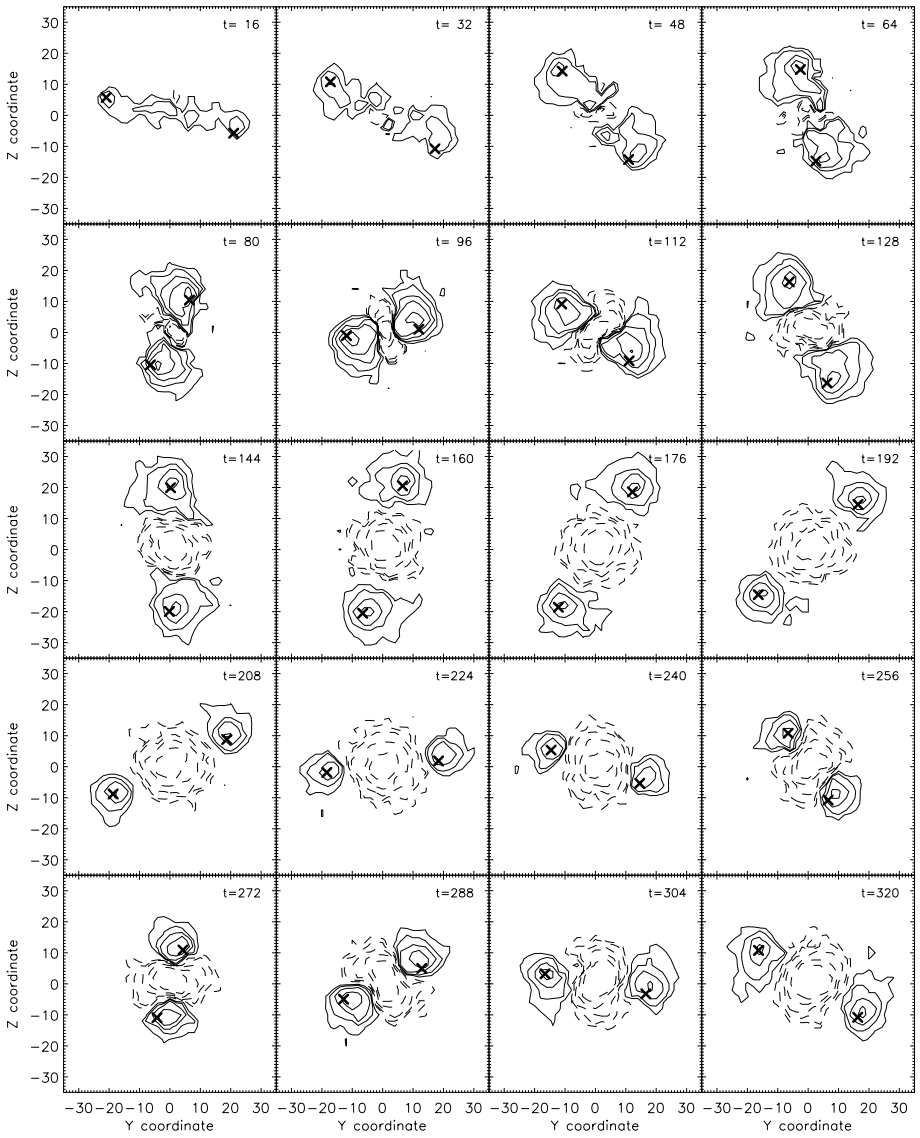

Figure 4. Wake in the halo, calculated directly from the particle density in the halo at different time-steps. For this plot only the particles in a slice of 1 disc scalelength centred on the satellite plane were considered. The contours are overdensities and underdensities with respect to the unperturbed halo model. To suppress particle noise, we smoothed these maps to a resolution of 6 scalelengths. The positions of the satellites are given by the crosses. See Section 3.4 for details on the imaging of the wake.

of 6° with a satellite of 1.5×10^{11} $M_{\odot}$, the amplitude of the warp that a LMC-like satellite (1.5×10^{11} $M_{\odot}$) is going to generate on the Galaxy is not going to be greater than 0.6°. This is a conservative upper limit, taken into account that we know that the halo noise generates a considerable percentage of this quantity.

3.6 Full simulation

In this section we take into account the effect that the gravity of the disc has on the halo, and the backreaction of the halo on the disc. We also consider the effect of the halo on the satellite, causing its orbit to spiral inwards by dynamical friction. The satellite we use in this simulation is as massive as that in simulation no 5, but its decaying orbit has been calculated with a satellite with the mass of the LMC, to avoid rapid decay of the orbit in an unrealistically short period of time. For the halo, we have used the relaxed King model halo described in Section 2.2.

We have carried out two simulations with these settings. The first of them (simulation no 8) is a control simulation with no satellite to determine the effect of halo particle noise in our disc. The disc in this simulation does not develop a more or less coherent warp as in simulation 1 (control simulation without backreaction). Instead, the inclination of the rings fluctuates fast and the line of nodes changes drastically with radius. At the end of the simulation ($t = 320$) the outer rings are inclined by 2.°5 (but showing no coherent warp).

Now we introduce the satellites (simulation no 9) to see how the influence of the disc on the halo will influence the warp. The first difference we observe in the evolution of the disc is that in this simulation the inclination of the inner parts is smaller than in previous simulations. This is caused by the fact that the halo is now flattened in the vicinity of the disc owing to the potential of the disc, and this creates a preferred plane (Dubinski & Kuijken 1995). In previous simulations a slight asymmetry in the initial halo can cause the inner disc to tilt with respect to the $z = 0$ plane. The

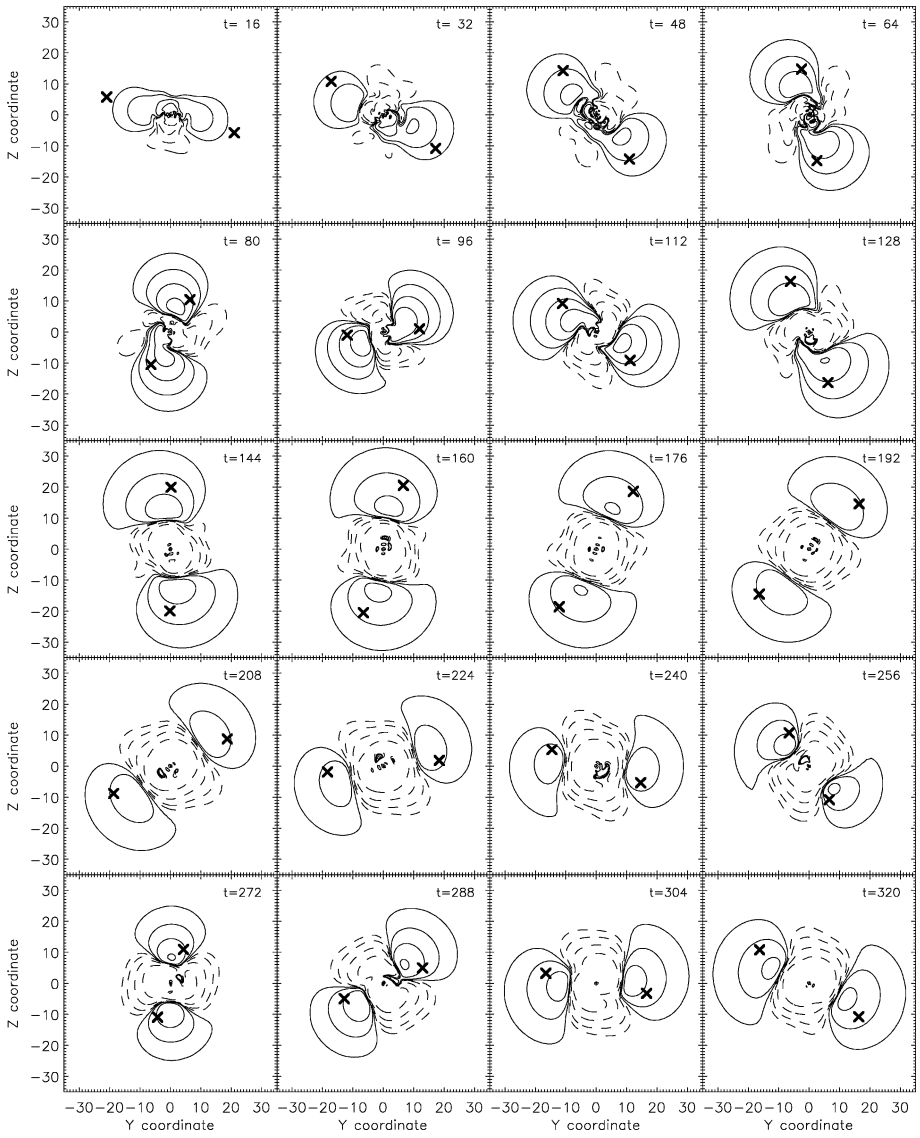

Figure 5. Wake in the halo, as calculated from the SCF code with terms up to $n = 6$, $l = 4$. The contours are overdensities and underdensities with respect to the unperturbed halo model, and have been calculated in the orbital plane of the satellite. See Section 3.4 for details on the imaging of the wake.

flattening of the halo now exerts a torque on the disc in the direction of the line of nodes of the warp, besides the torque caused by the wake created by the satellite. A flattened halo would have the same consequences in the previous simulations.

We also note that the warp has lost most of its coherence. The line of nodes is tightly wound up, smearing out the growing warp pattern, consistent with the simulations in Binney et al. (1998). A warp like this would be much more difficult to detect observationally than the warps we were getting without considering the backreaction of the halo on the disc. The amplitude of the warp is somewhat higher than in simulations nos 6 and 7, owing to the fact that the satellites are now affected by dynamical friction and this carries them closer to the disc, increasing their tidal force on it.

3.7 Summary of results

We have simulated the effect that a satellite has on a halo (wake), and the torque that this wake exerts on a disc. The wake amplifies the direct tidal field arising from the satellite, making larger warps than when this contribution is ignored. Our simulations show that this amplification is not larger than 25 per cent. Weinberg (1998) used the matrix method to follow the evolution of the satellite and the halo and obtained amplifications up to 500 per cent depending on the halo density profile. We have made extensive tests to check that our code can describe the wake in the halo accurately and we are unable to obtain such high amplifications. When we follow the evolution of a disc under the influence of the satellite and the halo we obtain warps that are not larger than 0.6° for the Galaxy–LMC system (using the maximum mass estimate for the LMC), while the observed Galactic warp is of the order of 4°.

4 ORIENTATION OF THE LINE OF NODES OF THE WARP

In addition to the simulations, it is possible to describe by means of a simple analytical model the global response of a disc–halo system

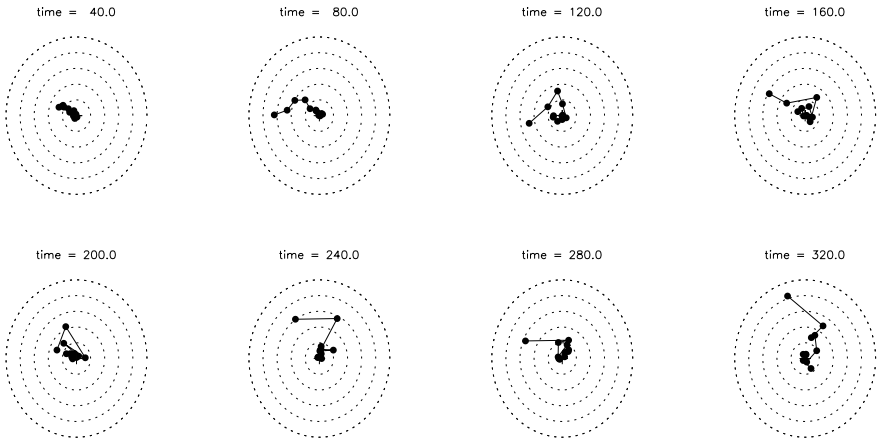

Figure 6. tip-LON diagrams at different time-steps for the simulation no 6. We have binned the disc every 0.5 scalelengths in radius. There is a dotted circle every degree.

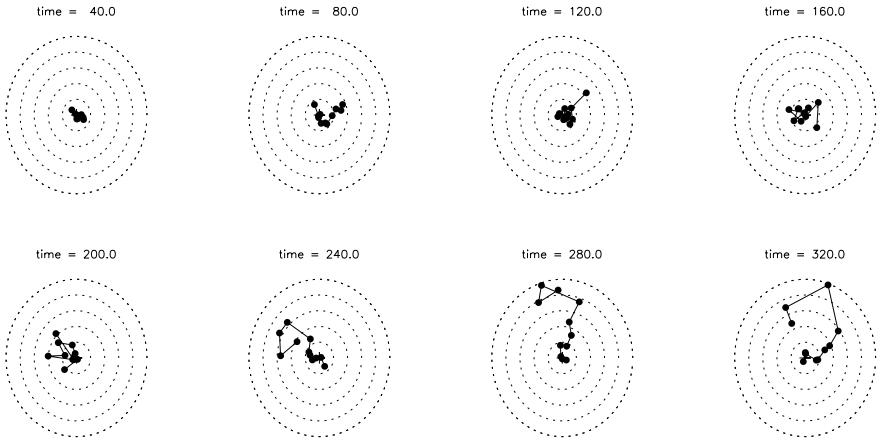

Figure 7. tip-LON diagrams at different time-steps for the simulation that has the same parameters as that in Fig. 6 except that the satellite is orbiting in the opposite sense (simulation no 7). We have binned the disc every 0.5 scalelengths in radius. There is a dotted circle every degree.

to a satellite. Though very simplified, such models can provide a useful indication of the amplitude and orientation of the warps that may be expected. As we show below, the orientation of the line of nodes can, in particular, already place useful constraints on the orbit a satellite would need to have to cause the warp.

In this section we consider such a simple analytic model, and use it to determine the orientation of the line of nodes of a warp generated by an orbiting satellite in a nearly polar orbit. We then use our code to test those predictions. In this whole section the effect that the bending of the disc on the halo, and its feedback on to the disc, are neglected. Later we will discuss the implications of this important assumption.

4.1 Analytic results with a simplified model

Consider a rigid disc, embedded in a rigid halo potential, and subjected to the potential of an orbiting satellite. The evolution of the disc is governed by the combined torque from the halo and the satellite. A stellar or gaseous disc is floppy, and so will warp when tilted, since it is not able to generate the stresses that would be required to keep it flat; however, the overall re-alignment of the disc angular momentum should be comparable between the rigid and floppy cases.

Fig. 8 illustrates the angles related to the satellite, and the definition of our coordinate system. The tilting of the disc (θ) is measured by the angle between the z-axis and the angular momentum of the disc.

The Lagrangian for a rigidly spinning, axisymmetric object is

$$\mathcal{L} = \frac{1}{2} I_1(\dot{\theta}^2 + \dot{\phi}^2 \sin^2\theta) + \frac{1}{2} I_3(\dot{\phi}\cos\theta + \dot{\psi})^2 - V(\theta, \phi), \qquad (1)$$

where (θ, ϕ, ψ) are the Euler angles, and I_3 and I_1 are the moments of inertia of the object about its axis of symmetry and about orthogonal directions. V is the potential energy of the body in the halo plus satellite potential. The ψ-equation of motion leads to the conserved quantity $S = I_3(\dot{\phi}\cos\theta + \dot{\psi})$, the spin. And for small deviations from the equator ($\theta = 0$), we can expand the other two equations in terms of $\xi = \sin\theta\cos\phi \simeq \theta\cos\phi$, $\eta = \sin\theta\sin\phi \simeq \theta\sin\phi$ (see Appendix A). The variables ξ and η are the x and y components of the normal vector of the disc.

If we consider a satellite in a polar circular orbit in the $x = 0$ plane, $\theta_S = \Omega_S t$, $\phi_S = 90^\circ$, the solution to the equations of motion is (see Appendix A)

$$\xi = \frac{2\Omega_S S}{\Delta} V_S \cos 2\Omega_S t; \quad \eta = \frac{4I_1\Omega_S^2 - V_H}{\Delta} V_S \sin 2\Omega_S t \qquad (2)$$

plus free precession and nutation terms, where $\Delta = (V_H - 4I_1\Omega_S^2)^2 - 4\Omega_S^2 S^2$. (A more general quasiperiodic satellite orbit yields a solution that can be written as a sum of such terms.) Note that the

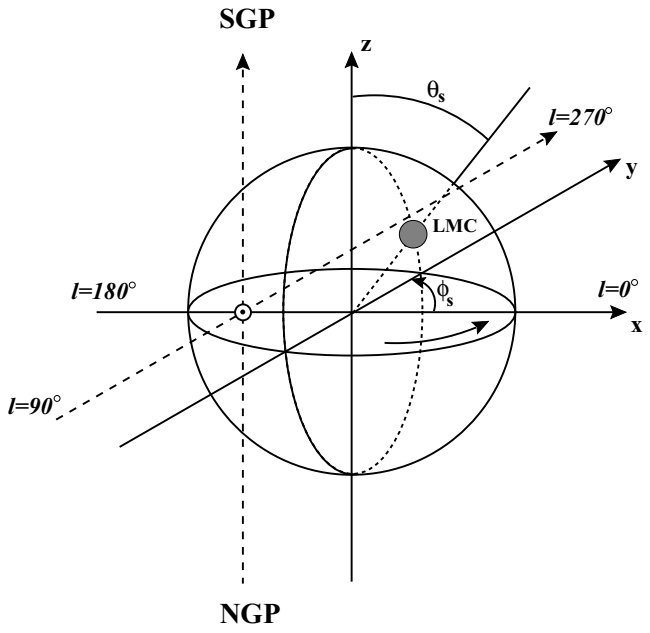

Figure 8. Definition of the coordinate system, satellite angles and orientation of the disc of the Galaxy. The disc lies on the $z=0$ plane. The Sun is on the left, and the galactic plane is viewed from the South Galactic Pole so that the disc rotates counterclockwise (indicated by an arrow). The angular momentum of the satellite points in the opposite direction to the x-axis.

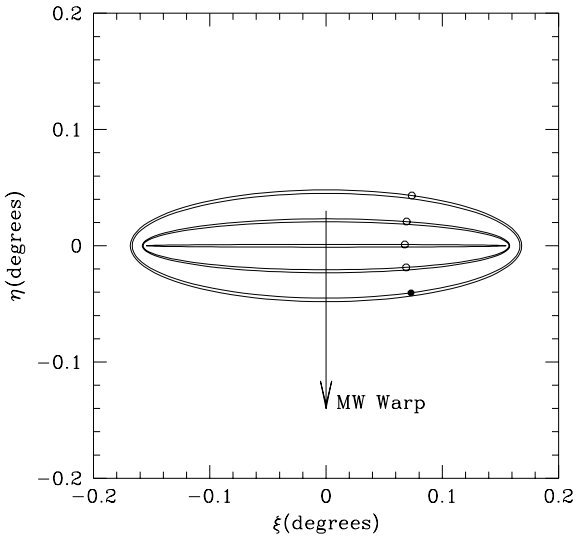

Figure 9. The oscillation of the axis of a rigid exponential disc subjected to the tidal field of an orbiting satellite. The amplitude is calculated assuming a satellite of mass 1.5×10^{10} $M_\odot$, orbiting at radius 50 kpc in the $z=0$ plane. The direction of the tilt of the Galactic disc with respect to the orbital plane of the Magellanic Clouds is indicated by the arrow. The dots mark the expected position of the disc axis given the current phase of the LMC orbit for (bottom to top) halo potential ellipticities $\epsilon=0$ (solid symbol), 0.05, 0.1, 0.15 and 0.2 (open circles).

satellite provokes an elliptical precession about the halo axis of symmetry, with axis ratio dependent on the halo flattening and on the satellite orbit frequency. For example, for an exponential disc of mass M, scalelength h and with a flat rotation curve of amplitude v, $I_3=2I_1=6Mh^2$ and $S=2hvM$. For such a disc in a spherical (or absent) halo ($V_{\rm H}=0$), a satellite orbiting at radius $r_{\rm S}$ has frequency $\Omega_{\rm S}=v/r_{\rm S}$, and hence the axis ratio of the forced precession is $(\xi:\eta)=r_{\rm S}/3h$. Hence the response of the disc to a distant satellite is mainly to nod perpendicular to the satellite orbit plane. This result can be understood as the classic orthogonal response of a gyroscope to an external torque: a distant satellite has a sufficiently low orbital frequency that the disc responds as if the torque were static.

For a slightly flattened potential of the form $\frac{1}{2}v^2\ln\{R^2+[z/(1-\epsilon)]^2\}$, $V_{\rm H}=Mv^2\epsilon$ (see Appendix C). With non-zero ϵ, the axis ratio of the precession cone becomes $[(4h/r_{\rm S})/(\epsilon-12h^2/r_{\rm S}^2)]$: again the oscillation in ξ is larger than that in η except for very flattened haloes.

The amplitudes generated by tidal perturbation from a satellite such as the LMC are small (less than a degree). The largest amplitude of oscillation is in the ξ-direction. The potential energy of the disc caused by the tidal field of the satellite can be shown to be (see Appendix B)

$$V_{\rm S}=\frac{3GM_{\rm S}I_1}{2r_{\rm S}^3}. \tag{3}$$

Hence equation (2) yields, to leading order in $h/r_{\rm S}$, an ξ-amplitude of

$$\frac{9}{8}\frac{GM_{\rm S}}{v^2r_{\rm S}}\frac{h}{r_{\rm S}}\simeq0.15^\circ \tag{4}$$

for the LMC (orbital radius of about 50 kpc and $r_{\rm S}/h\simeq11$). This number increases only slightly (a factor of 2) for halo flattenings up to 0.2 (see Fig. 9).

It is clear from this calculation that simple tidal tilting of a disc by an LMC-like satellite does not provide a good model for the warping in the Galaxy, because the orientation of the warp is not perpendicular to the orbital plane of the LMC. This constraint is independent of the strength of the perturbation $V_{\rm S}$.

The amplitudes are also much too small, but we have only considered the tilting of a rigid disc, and the situation can change when the floppiness of the disc is considered.

4.2 Simulation details

To test this scenario, and in particular to get beyond the rigid tilting considered above, we have performed some N-body simulations. We take the halo to be a background potential that does not respond to the disc or the satellite. It has been extensively shown (Nelson & Tremaine 1995; Dubinski & Kuijken 1995; Binney et al. 1998; Weinberg 1998) that the halo responds to changes in the potential caused by a warping disc or an orbiting satellite. In the case of the wake created by the warping disc the main effect is to damp the warp. This damping, though fast, happens on a time-scale that is slower than the precession frequency S/I_3, and so does not generate a phase shift in the disc tilt. In the case of the satellite, the wake created on the halo is roughly in phase with the satellite, so here too, we expect the orientation of the total tidal field felt by the disc to remain very similar.

We have performed simulations with two types of discs: a rigid disc and an exponential disc. The rigid disc run tells us how good the analytic predictions are, and the exponential disc is used later for a more realistic approach. The halo, disc and satellite models used are described in Section 2.2, and the code in Section 2.1. The mass of the satellite is $M_{\rm sat}/M_{\rm LMC}=1$

The first run was made with a satellite in a circular orbit, to try to reproduce the predictions in Section 4.1. Later the non-circular orbit described in Section 2.2 is used for the satellite, to analyse the consequences of the non-circularity of the orbit of a satellite.

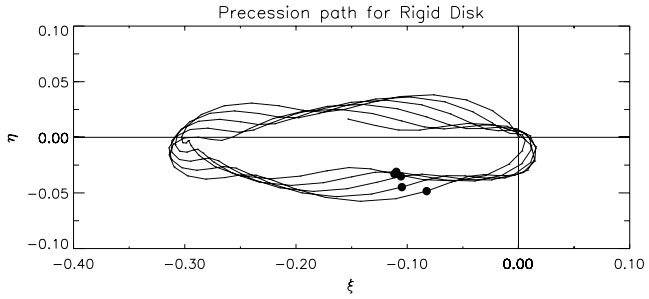

Figure 10. Precession path followed by the rigid disc: $\xi = \theta \cos\phi$, $\eta = \theta \sin\phi$ (in degrees). The dots indicate the state of the disc when the satellite has the same orbital phase as the LMC.

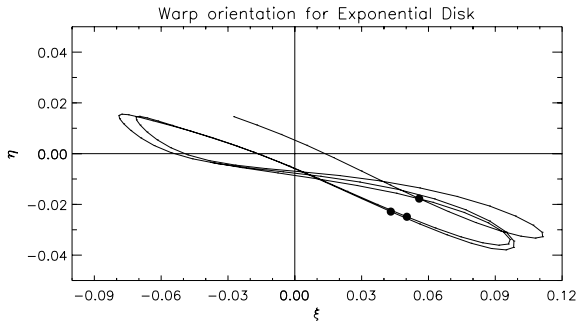

Figure 11. Warp orientation followed by the exponential disc: $\xi = \theta \cos\phi$, $\eta = \theta \sin\phi$ (in degrees). The dots indicate the state of the disc when the satellite has the same orbital phase as the LMC.

4.3 Rigid disc

As a first approach, we have evolved a rigid disc and analysed its evolution under the influence of an orbiting satellite. The result of our simulation is in good agreement with the analytic predictions. The disc wobbles under the influence of the satellite, describing an ellipse elongated in the direction perpendicular to the orbital plane of the satellite. The path followed by the disc is plotted in Fig. 10, where it can be seen that most of the time the maximum of the warp is located in the direction perpendicular to the orbital plane of the satellite. The ellipse is not as regular as in Fig. 9 for two reasons: the assumption that the disc is much smaller than the orbital radius of the satellite is not completely fulfilled; and there are some transient terms present because of the initial conditions of the simulation. This is also the cause for the precession ellipse of the disc not being centred on the origin.

The position of the warp when the satellite is at the location of the LMC is indicated by the dots in Fig. 10, and their location resembles the predicted one in Fig. 9 (for $\epsilon_{\rm halo} = 0$) remarkably well.

4.4 Exponential self-gravitating disc

We now consider a more realistic disc: an exponential disc model, in which we have also considered the self-gravity of the disc. The first thing that draws our attention in this simulation is a peak we see in the inclination at around 6.5 scalelengths. Simulations performed with a different rotation curve showed that this peak occurs at the locations on the disc that satisfy $\Omega_s / w_z = 2, 3, \ldots$, which are caused by resonances with the orbital frequency of the satellite.

This is not the kind of warp we are looking for, owing to the fact that it is the result of a satellite with a single frequency, and in the real case the eccentric orbit of the satellite will wash out this peak. Looking at the evolution of the disc it is clear that the warp loses its coherence at a radius of about 4.5 scalelengths (at a larger radius the line of nodes winds up), so we will measure the warp properties considering that the disc finishes there.

In the case of a floppy disc it is not straightforward to define a single inclination and position angle. We have separated the disc into two components: the inner disc and the outer (warped) disc. The inner disc consists on the first 2 scalelengths, and remains practically flat during the simulation. The warping angle is then calculated as the angle between the inner and outer disc vectors. We have chosen to use the disc vectors and not the angular momentum, for example, not to penalize the outer less massive rings. The results presented here do not change significantly when the definition of the inner disc is altered.

It has to be borne in mind that the warping angles quoted here are different from the maximum amplitude of the warp, which is larger by a factor never greater than 5.

Using this method we obtain a plot similar to Fig. 10 for the exponential disc, which is shown in Fig. 11. Only the path after $t = 160$ is shown, which is the moment when the disc behaviour reaches an equilibrium.

Note that the predictions for the Galactic warp orientation do not change much when the floppiness of the disc is taken into account: it is clearly close to the direction perpendicular to the orbit of the satellite, as Section 4.1 predicted, and not aligned with it, as we observe in the Galaxy.

4.5 Non-circular orbit and flattened haloes

We also considered non-circular orbits, to allow for the fact that the orbit derived for the Clouds has a pericentre of 50 kpc and an apocentre of 100 kpc (Lin et al. 1995). The changing radius of the satellite causes a fluctuating tidal field amplitude, which could be important for the dynamics of the disc. Here we show that, in fact, the effect does not change our conclusions materially.

First, to gain an idea of what to expect, we integrated the analytic equations of Section 4.1 with a satellite in this kind of orbit. The result was, as before, that the precession path of the disc was contained within an ellipse, elongated along the direction perpendicular to the plane of the satellite. This causes the warp maxima to be close to the direction perpendicular to the orbit of the satellite most of the time.

We then performed simulations with this type of orbit. The first thing we observe in these simulations is that the resonance peak we found in the circular orbit simulation has disappeared. Now the satellite does not have a single frequency, so the result is not surprising. The energy of the resonance now gets distributed along different parts of the disc, and no coherent pattern can be maintained across the disc, winding up the outer parts of the disc. When we look at the inner 4.5 scalelengths as before, the precession pattern remains similar to the simulation with the circular orbit, so does the prediction of the longitude of the warp at the actual orbital phase of the LMC. So our conclusions are not modified by the non-circularity of the orbit.

The haloes considered in all of these simulations are spherical, which means that they do not contribute to the generation of torques on the disc. Galactic haloes are not spherical, which creates a preferred plane in which the disc settles. Ellipticities of the order of 0.05 in the potential make the precession paths described before yet

more elongated, which would make the chances of finding the warp maxima in the direction of the satellites even more unlikely.

4.6 Backreaction from the halo

The strongest assumption in this work is the assumption that the halo does not react to the warping of the disc, which will have a further influence on the warping disc. However, there are scenarios where this effect is not very important: in the case of galaxies with a minimal halo. In these systems, the line of nodes of the warp generated by a satellite in a polar orbit would be aligned with the orbit, and not at 90° to it. In the case of the Milky Way–LMC system this would mean that the line of nodes of the warp would be along $l \simeq 0°$–$180°$. The observed line of nodes for the galactic warp is approximately perpendicular to this direction. A similar prediction holds for MOND (Milgrom 1983).

5 CONCLUSIONS

We have been unable to reproduce Weinberg's prediction Weinberg (1998) of strong tidal amplification of a disc warp by the gravitational wake of a satellite. In the case of the Milky Way–LMC system this factor has to be at least a factor of 5, and we find amplifications no higher than 25 per cent in the total torques and smaller than 20 per cent in warp amplitude. This amplification is achieved for the halo profile and satellite parameters that had a maximum amplification in the calculations by Weinberg (1998). It is possible that some halo profiles, together with specific satellite orbits may increase this amplification somewhat, but we have found no evidence that the tidal field from a satellite can be amplified as much as 500 per cent by means of the halo. We have tried several different simulation techniques, with large and varying number of particles, and consistently find evidence for only weak tidal field amplifications.

The reason for the difference with Weinberg (1998) is not clear to us. There are detailed differences between the models we used (in the exact bulge–halo mass profile, and in the shape of the disc mass distribution). Perhaps these differences are sufficient to affect the degree of warping by a factor of 5, but in any event our results indicate that this mechanism for warping relies on a rather delicate resonance, rather than being the result of a generic large amplification of satellite-induced halo wakes. As an explanation for warps as a universal phenomenon, therefore, this scenario still has problems.

We conclude from our simulations that the amplitude of the warps generated with LMC-like satellites is likely to be much lower than what is observed in the Galaxy. Assuming a high mass for the LMC, the typical inclination angles from the plane defined by the inner part of the disc are of the order of 0.6° (or less), which is a factor of 5 less then in the Galaxy. Furthermore, the line of nodes of the resulting warp is tightly wound. If smaller mass estimates for the Clouds are used (Meatheringham, Dopita & Ford Webster 1988), the results are even more discouraging. So, although periodic forcing of disc warps by tidal fields of orbiting satellites would appear to circumvent many of the persistence problems of other tidal field models for warps, we conclude that in the case of the Galaxy this does not appear to be a feasible model. Calculations using MOND would predict a larger warp amplitude for the Galaxy, but the predicted orientation of the warp (perpendicular to the observed one) would still hold.

Even if a halo is able to amplify the satellite tidal field (though the extent to which this happens may depend quite subtly on the halo structure), it will also strongly perturb the disc precession that accompanies the warping. Dubinski & Kuijken (1995) and Nelson & Tremaine (1995) showed that most realistic halo mass distributions damp the precession strongly, while Binney et al. (1998) showed that in the process the line of nodes of the warp winds up very fast, effectively destroying the forming integral-sign warp. Obtaining the amplification of the tidal field without the accompanying damping of the disc precession would seem to require haloes that are present at large radii, but not near the gyration radius of the disc, otherwise the disc would be too tightly coupled to the inner halo.

Our results thus suggest that the explanation for warps should be sought elsewhere. Either there is a frequently occurring, and presumably quite gentle, dynamical instability of disc–halo systems that has been overlooked so far, or an entirely different mechanism needs to be considered. Possibilities include late cosmic infall that continuously realigns the angular momentum vector of galaxies (Ostriker & Binney 1989), or a generic misalignment between disc and halo angular momentum vectors that may excite warps (Debattista & Sellwood 1999).

REFERENCES

Barnes J., Hut P., 1986, Nat, 324, 446
Binney J., Jiang I., Dutta S., 1998, MNRAS, 297, 1237
Bosma A., 1991, in Casertano S., Sackett P.D., Briggs F., eds, Warped Discs and Inclined Rings Around Galaxies. Cambridge Univ. Press, Cambridge, p. 181
Briggs F., 1990, ApJ, 352, 15
Burke B.F., 1957, AJ, 62, 90
Debattista V.P., Sellwood J.A., 1999, ApJ, 513, L107
Dubinski J., 1996, New Astron., 1, 133
Dubinski J., Kuijken K., 1995, ApJ, 442, 492
Hernquist L., Ostriker J.P., 1992, ApJ, 376, 375
Hunter C., Toomre A., 1969, ApJ, 155, 747
Ing-Guey J., Binney J., 1999, MNRAS, 303, L7
Kerr F.J., 1957, AJ, 62, 93
Kuijken K., 1997, in Persic M., Salucci P., eds, ASP Conf. Ser. Vol. 117, Dark and Visible Matter in Galaxies. Astron. Soc. Pac., San Francisco, p. 220
Kuijken K., Dubinski J., 1995, MNRAS, 227, 134
Lin D.N.C., Jones B.F., Klemola A.R., 1995, ApJ, 439, 652
Lynden-Bell D., 1985, in van Woerden H., ed., The Milky Way Galaxy. Reidel, Dordrecht, p. 461
Meatheringham S.J., Dopita M.A., Ford Webster B.L., 1988, ApJ, 327, 651
Milgrom M., 1983, ApJ, 270, 365
Nelson R.W., Tremaine S., 1995, MNRAS, 275, 897
Ostriker E.C., Binney J.J., 1989, MNRAS, 237, 785
Sancisi R., 1976, A&A, 53, 159
Sánchez-Saavedra M.L., Battaner E., Florido E., 1990, MNRAS, 246, 458
Schommer R.A., Olszewski E.W., Suntzeff N.B., Harris H.C., 1992, AJ, 103, 447
Sparke L.S., Casertano S., 1988, MNRAS, 234, 837
Toomre A., 1983, in Athanassoula E., ed., Proc. IAU Symp. 100, Internal Kinematics & Dynamics of Galaxies. Reidel, Dordrecht, p. 177
Weinberg M.D., 1998, MNRAS, 299, 499

APPENDIX A: MOTION OF A RIGID DISC EMBEDDED IN A HALO UNDER THE INFLUENCE OF A SATELLITE

The Lagrangian for a rigidly spinning, axisymmetric object is

$$\mathcal{L} = \frac{1}{2} I_1(\dot\theta^2 + \dot\phi^2 \sin^2\theta) + \frac{1}{2} I_3(\dot\phi\cos\theta + \dot\psi)^2 - V(\theta,\phi), \qquad \text{(A1)}$$

where (θ, ϕ, ψ) are the Euler angles, and I_3 and I_1 are the moments of inertia of the object about its axis of symmetry and about

orthogonal directions. V is the potential energy of the body in the halo plus satellite potential. The ψ-equation of motion leads to the conserved quantity $S = I_3(\dot{\phi}\cos\theta + \dot{\psi})$, the spin, and the other two equations of motion then become

$$I_1\ddot{\theta} - I_1\dot{\phi}^2\sin\theta\cos\theta + S\dot{\phi}\sin\theta + \frac{\partial V}{\partial\theta} = 0 \tag{A2}$$

and

$$I_1\frac{\mathrm{d}}{\mathrm{d}t}(\dot{\phi}\sin^2\theta) + \frac{\partial V}{\partial\phi} = 0. \tag{A3}$$

For small deviations from the equator ($\theta = 0$), we can expand these equations in terms of $\xi = \sin\theta\cos\phi \simeq \theta\cos\phi$, $\eta = \sin\theta\sin\phi \simeq \theta\sin\phi$. In these terms the equations of motion become

$$I_1\ddot{\xi} + S\dot{\eta} + \frac{\partial V}{\partial\xi} = 0, \tag{A4}$$

$$I_1\ddot{\eta} - S\dot{\xi} + \frac{\partial V}{\partial\eta} = 0. \tag{A5}$$

For small ξ, η, the potential energy of the disc owing to the flattened halo will have the form $\frac{1}{2}V_{\rm H}(\xi^2+\eta^2)$, and that owing to the satellite at position $\theta_{\rm S}, \phi_{\rm S}$ will be $-V_{\rm S}(\sin^2\theta_{\rm S} - \xi\sin 2\theta_{\rm S}\cos\phi_{\rm S} - \eta\sin 2\theta_{\rm S}\sin\phi_{\rm S})$, where $V_{\rm H}$ and $V_{\rm S}$ are constants representing the strengths of the halo torque and of the quadrupole of the tidal field from the satellite, respectively (see Appendices B and C). Hence we find

$$I_1\ddot{\xi} + S\dot{\eta} + V_{\rm H}\xi + V_{\rm S}\sin 2\theta_{\rm S}\cos\phi_{\rm S} = 0, \tag{A6}$$

$$I_1\ddot{\eta} - S\dot{\xi} + V_{\rm H}\eta + V_{\rm S}\sin 2\theta_{\rm S}\sin\phi_{\rm S} = 0. \tag{A7}$$

If furthermore the satellite orbit is circular and polar in the $x = 0$ plane, $\theta_{\rm S} = \Omega_{\rm S}t$, $\phi_{\rm S} = 90^\circ$, and the solution to the equations of motion is

$$\xi = \frac{2\Omega_{\rm S}S}{\Delta}V_{\rm S}\cos 2\Omega_{\rm S}t; \quad \eta = \frac{4I_1\Omega_{\rm S}^2 - V_{\rm H}}{\Delta}V_{\rm S}\sin 2\Omega_{\rm S}t \tag{A8}$$

plus free precession and nutation terms, where $\Delta = (V_{\rm H} - 4I_1\Omega_{\rm S}^2)^2 - 4\Omega_{\rm S}^2S^2$.

APPENDIX B: POTENTIAL OF AXISYMMETRIC DISC OWING TO A SATELLITE

The potential energy of a disc of surface density $\Sigma(r)$ and in the gravitational field owing to a satellite at position $\boldsymbol{r}_{\rm S}$ is given by

$$V = -\int \mathrm{d}^2\boldsymbol{r}\,G\Sigma(r)\frac{M_{\rm S}}{|\boldsymbol{r} - \boldsymbol{r}_{\rm S}|}. \tag{B1}$$

Choosing spherical coordinates for the position of the satellite (see Fig. 8), and Cartesian coordinates in the disc plane so that the satellite has $x = 0$, we have

$$V = -GM_{\rm S}\int \Sigma\,\mathrm{d}x\,\mathrm{d}y\left(r_{\rm S}^2 - 2yr_{\rm S}\sin\theta_{\rm S} + x^2 + y^2\right)^{-1/2}. \tag{B2}$$

Assuming that the disc is small compared with $r_{\rm S}$, we can expand the integrand in x and y. For an axisymmetric disc the second-order terms are the first ones that generate a potential gradient: they are

$$V = -\frac{GM_{\rm S}}{r_{\rm S}^3}\int \Sigma\,\mathrm{d}x\,\mathrm{d}y\left[-\frac{1}{2}\left(1 - 3\sin^2\theta_{\rm S}\right)y^2 - \frac{1}{2}x^2\right] \tag{B3}$$

which results in

$$V = -\frac{3GM_{\rm S}I_1}{2r_{\rm S}^3}\sin^2\theta_{\rm S} + \text{constant}. \tag{B4}$$

Now, the angle $\theta_{\rm S}$ is defined as the scalar product of the position vector of the satellite with the vector normal to the disc ($\cos\theta_{\rm S} = \boldsymbol{r}_{\rm S}\boldsymbol{n}_{\rm d}$). If we express the normal vector of the disc as $\boldsymbol{n}_{\rm d} = (\xi, \eta, 1 - \sqrt{\xi^2+\eta^2})$, then we obtain that for small inclinations the potential of a tilted disc owing to an orbiting satellite is

$$V = -\frac{3GM_{\rm S}I_1}{2r_{\rm S}^3}\left(\sin^2\theta_{\rm S} - \xi\sin 2\theta_{\rm S}\cos\phi_{\rm S} - \eta\sin 2\theta_{\rm S}\sin\phi_{\rm S}\right) + \text{constant}. \tag{B5}$$

APPENDIX C: POTENTIAL OF AN AXISYMMETRIC DISC OWING TO A HALO

The potential energy V of a disc with surface density $\Sigma(r)$ and total mass M, inclined at an angle θ with respect to the equatorial plane $z = 0$ of an axisymmetric halo with potential $V_{\rm halo}(R, z)$ is

$$V = \int_{r=0}^{\infty} r\,\Sigma(r)\,\mathrm{d}r\int_{\phi=0}^{2\pi} V_{\rm halo}\left[(r^2 - r^2\sin^2\theta\sin^2\phi)^{1/2}, \times r\sin\theta\sin\phi\right]\mathrm{d}\phi. \tag{C1}$$

For a flattened logarithmic potential of the form $V_{\rm halo} = -\frac{1}{2}v^2\ln\{R^2 + [z/(1-\epsilon)]^2\}$, and assuming that the flattening of the halo and the departure of the disc from the $z = 0$ plane are small ($\epsilon, \theta \ll 1$) we obtain that

$$V = \frac{1}{2}Mv^2\epsilon\sin^2\theta. \tag{C2}$$

In terms of $\xi = \sin\theta\cos\phi$, $\eta = \sin\theta\sin\phi$ this becomes

$$V = \frac{1}{2}V_{\rm H}(\xi^2 + \eta^2), \tag{C3}$$

where $V_{\rm H} = Mv^2\epsilon$.

This paper has been typeset from a TEX/LATEX file prepared by the author.